Indian Journal of Chemistry
Vol. 62, July 2023, pp. 714-719
DOI: 10.56042/ijc.v62i7.3827

Schiff base metal complexes: Synthesis, characterisation, and antibacterial properties

Madhukar Vainala[a], Sunkari Jyothi*[a] & Sriramoju Shamili[b]

[a] Department of Chemistry, Kakatiya University, Warangal 506 009, India

[b] Department of Chemistry, Vaagdevi Degree and PG College, Hanamkonda 506 001, India

E-mail: vainalamadhu2010@gmail.com

Received 01 August 2022; accepted(revised) 20 June 2023

Five novel metal complex derivatives from the 2N-salicylidene-5-(*p*-amino phenyl)-1,3,4-thiadiazole (HL) in alcoholic medium have been effectively synthesised by combining HL with the metal ions Vo(II), Co(II), Rh(III), Pd (II) and Au(III). Except for the Vo(II) and Co(II) complexes, which have square pyramidal and tetrahedral geometries, all of the complexes have a monomeric structure, with the metal centre moieties being four-coordinated. HL has been shown to be more effective *in vitro* against the tested bacteria and complexes **1–5** have been found to have greatest antibacterial activity relative to the standard antibiotic (Kanamycin).

Keywords: Schiff bases, Metal complexes, *In vitro* antibacterial activity

Schiff bases, ligands that bind to metal ions through the coordination of azomethine amine, are made up of amino and carbonyl compounds. C-N linkage is essential in azomethine derivatives, which have antibacterial, antifungal, cancer-fighting and antimalarial activities[1]. Some of the 1,3,4-thiadiazole compounds have fascinating biological properties. They are presumably active because of the intense aromaticity, stability and long-term viability of this ring-based system, a lack of toxicity for higher vertebrates, including humans[2]. Incorporating functional groups that interact with biological receptors into this ring produces molecules with exceptional features[3]. If we exclude the no longer clinically utilised, but historically significant antibacterial sulfonamides (albucid and globucid), the most fascinating examples are 5-amino-l,3,4-thiadiazole derivatives[4]. These new Schiff base thiadiazole compounds may interact with various metal ion moieties in order to better understand their characteristics. Consequently, the structural-activity connection investigation of 1,3,4-thiadiazoles might develop in the near future.

The synthesis and characterization of new complex derivatives of 2N-salicylidene-5-(*p*-nitro phenyl)-1,3,4-thiadiazole could be extensively studied by coordinating to various metal ion moieties[5]. In continuation interest of this study of transition metal complexes, these new 2N-salicylidene-5-(p–amino phenyl)-1,3,4–thiadiazole (HL) complex compounds are described earlier[6]. This work also includes preliminary *in vitro* antibacterial screening results for the complexes generated[7]. In the present work, the ligand HL's oxygen and nitrogen atoms were employed to coordinate five separate metal ions, yielding the corresponding complexes. Except for complexes **2** and **3**, all of the complexes were four-coordinated. The complexes **1–5** were found to have greatest antibacterial activity relative to the standard antibiotic (Kanamycin).

Experimental Section

General and instrumental

The reagents, starting materials, and solvents were all purchased commercially and used without further purification. A Gallen Kamp melting point device with a hot stage was used to measure the melting points. Analysis of elements C, H, N, and S was carried out on a Fison EA 1108 spectrograph. The FTIR spectra were collected in the frequency range of 4000–200 cm^{-1} using an FTIR 8300 Shimadzu Spectrophotometer and a CsI disc. The Shimadzu UV–Vis. 160 A-Ultraviolet Spectrophotometer was used to acquire the UV–Vis spectra in the 200–1100 nm range. The Magnetic Susceptibility Balance Bruke Magnet B.M.6 was used to measure the magnetic

susceptibility at RT. The atomic absorption was measured with a Shimadzu 680 cc flame and the conductivity was detected using a WTW conductivity metre. A Jeol 400 MHz spectrometer was used to record the ^{1}H and ^{13}C NMR spectra in the presence of deuterated d6-DMSO as the solvent and TMS as the internal standard. The Shimadzu QP-2010 mass spectrometer was used to examine the data, and the *m/z* was represented in elementary charge units using the ESI (70-eV) model with a direct intake probe.

Preparation of 2N-salicylidene-5-(*p*-amino phenyl)-1,3,4-thiadiazole, HL

For 3 h, a solution of 4-aminobenzoic acid (0.01 mol), thiosemicarbazide (0.01 mol), and phosphorus oxychloride (5 mL) was heated under reflux. After cooling, it was heated for another 4 h at reflux with 50 mL of distilled water. The filtrate was then neutralised with potassium hydroxide. In order to get 5-(4-aminophenyl)-1,3,4-thiadiazol-2-amine, the precipitate was rinsed with cold distilled water before being recrystallized in an ethanol-water solvent mix. To make the yellow precipitate, a solution of 5-(4-aminophenyl)-1,3,4-thiadiazol-2-amine and salicylaldehyde was heated for 3 h under reflux. Precise precipitation was obtained by filtration and crystallisation from the solution in ethanol in order to get the 2N sulfonyl-5-(*p*-aminophenyl)-1,3-thiadiazole ligand. Fig. 1 depicts the procedures involved in synthesising the ligand HL in a simplified manner.

Preparation of complexes

HL 2N-salicylidene-5-(*p*-amino phenyl)- 1,3,4-thiadiazole ethanol solution was treated with a 1:2 (metal:ligand) molar ratio of metal ions [$Vo(II)SO_4H_2O$, Co- $Cl_2.6H_2O$, $RhCl_3.XH_2O$, $PdCl_2$ and $HAuCl_3.H_2O$]. When the mixture was heated for 0.5 h under reflux, coloured precipitates were developed. It was then filtered, washed with distilled water, and then recrystallized from alcohol to remove the precipitates.

Results and Discussion

To synthesize the complexes, the metal salts were heated to their respective metal salts in the same 1:2 molar ratio under reflux. The TLC purity results were obtained in an earlier study for ligand, HL, and complexes **1–5** (Ref. 8). There is a high melting point for complexes **1–5**, which indicates that they were separated from more pure complexes[9]. The expected formula for complexes **1–5** was confirmed by micro-elemental analyses of the C, H, N, and S complexes, as well as their molecular weight[10]. The ligand, HL,

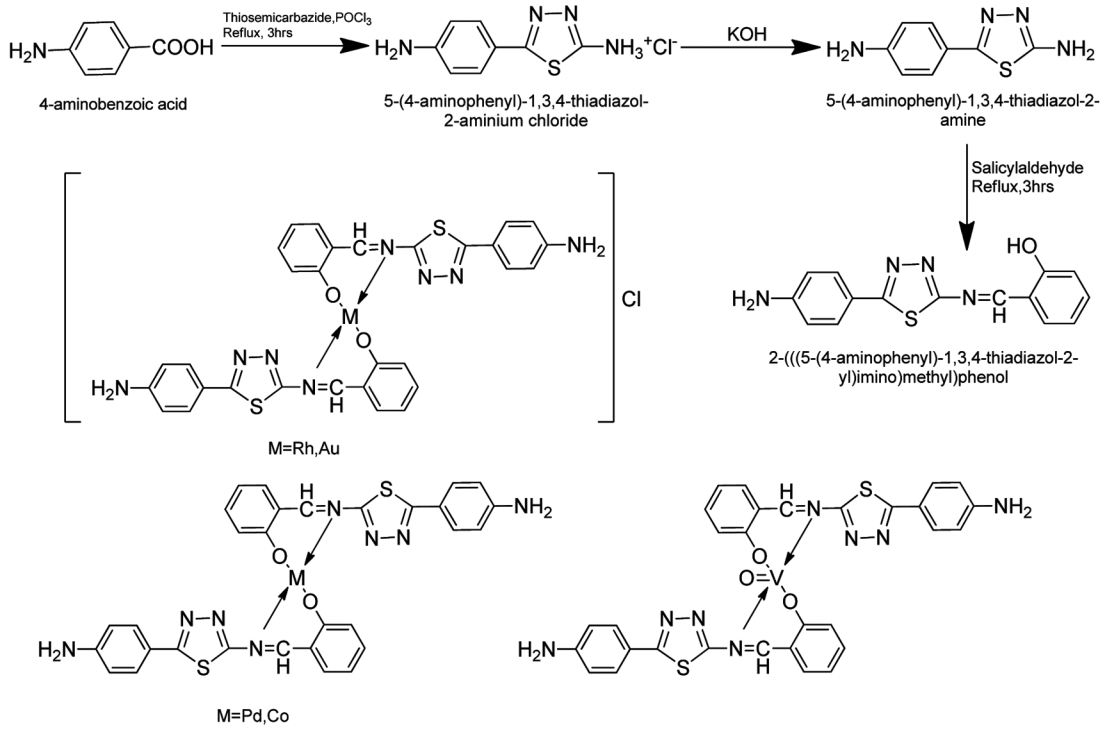

Fig. 1 — The structure of HL and the proposed structure of complexes **1-5** (M=metal).

Table 1 — Melting points, elemental analytical data (%) and *m/z* value of HL and complexes **1–5**

Compd	Physical Appearence	Melting Point (°C)	Elemental (%)				(M) metal	*m/z*
			C	H	N	S		
HL	Yellow	110–113	55.45 (55.24)	3.43 (3.26)	17.42 (17.22)	9.89 (9.68)	–	327.0
$Rh(L)_2$, **1**	Deep Orange	192–194	46.43 (45.45)	2.75 (2.68)	14.22 (14.27)	8.10 (8.20)	14.16 (14.02)	693.06
$Co(L)_2$, **2**	Blue	99–102	50.60 (50.73)	3.32 (3.20)	15.77 (15.80)	8.76 (9.13)	8.25 (8.38)	649.72
$VO(L)_2$, **3**	Green	208–210	50.43 (50.17)	3.03 (3.06)	15.85 (15.77)	9.43 (8.52)	9.63 (9.51)	590.07
$Au(L)_2$, **4**	Pale Yellow	210–213	40.67 (40.60)	2.80 (2.59)	12.22 (12.56)	7.41 (7.63)	22.42 (22.37)	787.06
$Pd(L)_2$, **5**	Brown	196–198	43.52 (47.37)	1.42 (2.80)	7.54 (14.96)	7.43 (8.64)	14.20 (14.03)	697.20

and the suggested structures for complexes **1–5** are shown together in Fig. 1. Table 1 provides the melting point, micro-element analysis, and *m/z* data[11] of the studied complexes.

In complexes **1–5**, HL exhibited separate stretching bands at 1635 and 1116 cm^{-1}, which were ascribed to the ligand's υ(CN) and υ(C–O) atoms, respectively. This indicates that the ligand, HL, was involved in the coordination of complexes **1–5**, which were discovered to have a lower υ(CN) number than their nitrogen atom. Oxygen and nitrogen atoms included in the ligand were found to be complexed with metal in the bands that ranged from 556 to 500 cm^{-1} and 488 to 432 cm^{-1}, respectively. For the ligand, HL, and the complexes **1–5**, the most important infrared data may be found in Table 2.

Table 3 shows the ligand, HL, and complexes **1–5** in ethanol solution's ultraviolet–visible electronic spectra. At 47,610, 39,360, and 28,911 cm^{-1}, the ligand displayed three distinct bands that were ascribed to π→π*, π→π*, and n→π* electronic transitions. As an additional snippet of information, it displayed the d-d electronic transition detected in the visible area for metal d orbitals for all complexes as well as the same electronic transition found in the ligand. An electronic transition band was seen in Vo(II) at 23,800 cm^{-1} assigned to the $^2B_2 \rightarrow {}^2A_1$ transition and Co(II) 6,225, 9,346 and 15,655 cm^{-1}, respectively, which was ascribed to $^4A_2 \rightarrow {}^4T_2{}^{(F)}$; $^4A_2 \rightarrow {}^4T_1{}^{(F)}$; $^4A_2 \rightarrow {}^4T_1{}^{(p)}$ transition respectively. The $^1A_{1g} \rightarrow {}^1B_{1g}$ and L (ligand) → Rh were shown to be responsible for the bands occurring at 23,210 and 26,323 cm^{-1} for Rh(III) (charge transfer, C.T.). To distinguish $^1A_{1g} \rightarrow {}^1B_{1g}$ from $^1A_{1g} \rightarrow {}^1E_g$ and from L→Pd (C.T.), three distinct bands were seen in the Pd(II) complex at 22,131 cm^{-1}, 24,500 cm^{-1}, and 31,110 cm^{-1}.

Another complex of Au(III) showed three bands in the visible area at 16,500, 24,022 and 30,540 cm^{-1}, which were assigned to $^1A_{1g} \rightarrow {}^3B_{1g}$, $^1A_{1g} \rightarrow {}^1B_{1g}$, $^1A_{1g} \rightarrow {}^1Eg$. A further confirmation of the complexation was provided by the ^1H NMR spectrum of complexes **1–5**. Complexes **1–5** did not have this prominent 9.90-ppm peak in their ^1H NMR spectrum, which indicated deprotonation and complexation of anion to metal ions. There were some similarities between the ^1H NMR spectra of complexes **1–5** and the ligand, HL, with –N=CH– and aromatic proton signals centred at δ≈7.26 ppm and ranging from 8.34–9.26 ppm, respectively. Carbon signals centred at δ≈112.11 ppm and thiadiazole carbon signals centred at δ≈87.61 and 90.69 ppm, respectively, found in the ^{13}C NMR analysis showed some similarities to the ligand HL in all the complexes. As a result, aromatic carbons of both complexes **1–5** and HL were found in the downfield area between 125.33 and 132.44 ppm. NMR spectra of ligand, HL, and complexes **1–5** are often free of unidentified peaks, which indicate the quality of the substances. Ligands, HLs, and complexes **1–5** are listed in Table 4 with their NMR spectra.

Table 2 — Selected infrared data of HL and complexes **1–5**

Compd	Wavelengths (cm^{-1})			
	υ (C=N)	υ (C-O)	υ (M-O)	υ (M-N)
HL	1645	1125	–	–
$Rh(L)_2$, **1**	1682	1115	508	486
$Co(L)_2$, **2**	1604	1122	506	483
$VO(L)_2$, **3**	1608	1114	519	476
$Au(L)_2$, **4**	1616	1124	514	486
$Pd(L)_2$, **5**	1614	1118	506	488

Table 5 lists the magnetic moments and conductivities of complexes **1–5** based on their magnetic moment and conductivity measurements. The partly filled d-orbital in these elements' outer shells contains unpaired electrons, which gives these elements their magnetic characteristics. The complex metal ions' electronic states may be inferred from these magnetic data. As a result, complex **1** was referred to as a paramagnetic structure, and the VO(II) metal core had a square pyramidal shape. No electrolyte is detected by conducting measurements.

Table 3 — Electronic spectral data of HL and complexes **1–5** in ethanol

Compd	Absorption bands (cm^{-1})	Assigned Transition
HL	47,610, 39,360, 28,911	π→π*, π→π*, n→π*
$Rh(L)_2$, **1**	39,673, 28,686 , 23,210, 26,323	π→π*,n→π*,$^1A_1g \rightarrow {}^1B_1g$,L→Rh(C.T)
$Co(L)_2$, **2**	39,670, 28,640, 6,225, 9,346, 15,655	π→π*,n→π*,$^4A_2 \rightarrow {}^4T_2{}^{(F)}$, $^4A_2 \rightarrow {}^4T_1{}^{(F)}$, $^4A_2 \rightarrow {}^4T_2{}^{(p)}$,
$VO(L)_2$, **3**	40,826, 28,633,23,820	π→π*, n→π*,$^2B_2 \rightarrow {}^2A_1$
$Au(L)_2$, **4**	42,025, 30,959,16,500, 24,022, 30,540 , 35,610	$^1A_1g \rightarrow {}^3B_1g$, $^1A_1g \rightarrow {}^1B_1g$, $^1A_1g \rightarrow {}^1Eg$, L→Au (C.T)
$Pd(L)_2$, **5**	39,667, 28,560 ,22,131, 24,500, 31,110	π→π*,n→π*,$^1A_1g \rightarrow {}^1B_1g$, $^1A_1g \rightarrow {}^1Eg$,L→Pd (C.T)

Table 4 — ^1H and ^{13}C NMR data of HL and complexes **1–5** in DMSO-d_6

Chemical shift δ (ppm)

	^1H NMR			^{13}C NMR		
Compd	-N=CH-	Aromatic	OH	-N=CH-	Thiadiazole	Aromatic
HL	7.26 (s)	8.34–9.26(m)	9.90	112.11	87.61, 90.69	125.33-132.44
$Rh(L)_2$, **1**	7.45 (s)	8.42–9.11(m)	–	110.40	87.64, 90.71	125.53–132.72
$Co(L)_2$, **2**	7.58 (s)	8.40–9.28(m)	–	112.82	87.65, 90.83	125.42–132.52
$VO(L)_2$, **3**	7.46 (s)	8.24–9.27(m)	–	114.65	87.66, 90.68	125.48–132.42
$Au(L)_2$, **4**	7.31 (s)	8.52–9.38(m)	–	120.47	87.66, 90.74	125.44–132.42
$Pd(L)_2$, **5**	7.66 (s)	8.23–9.40(m)	–	114.38	87.63, 90.74	125.62–132.57

Table 5 — Conductivity measurements and magnetic moment of HL and complexes **1–5** in DMF

Compd	Conductivity (μS/cm)	Magnetic moment (BM)	Proposed Structure
HL	–	–	–
$Rh(L)_2$, **1**	155	2.54	Square planar
$Co(L)_2$, **2**	16	0.86	Tetrahedral
$VO(L)_2$, **3**	22	1.78	Square pyramidal
$Au(L)_2$, **4**	175	1.68	Square planar
$Pd(L)_2$, **5**	142	1.56	Square planar

Complex **2** reported a magnetic moment of 0.86 B.M. and assumed that the Co(II) metal moiety had a tetrahedral geometry. The complex's molar conductivity in DMF shows it's non-electrolyte. Complex **3** shows 1.78 magnetic moment revealing a larger (d-orbital) contribution, and DMF conductivity measurements indicated the complex was conducting. Complex **4** is 1.56 B.M magnetic moment shows low spin. Non-ionicity was shown *via* DMF conductivity. Diamagnetic Complex **5** was conducting in DMF.

All complexes were examined in ethanol to determine the M/L ratio using Job's Method. A series of solutions were produced with 10^{-3} M of metal ion and ligand, HL. The M/L ratio was calculated by the connection between absorbed light and mole ratio of M/L. The metal to ligand, HL ratio was 1/2 for complexes **1–5**, identical to the solid state. According to the spectral analysis, complex **1** has square pyramidal geometry, complex **2** is tetrahedral, and the remaining three are square planar. Fig. 1 shows the suggested structures of complexes **1–5**.

The greatest genetic and metabolic variety may be found in microorganisms, which have been around for more than 3.8 billion years. Because of their critical function in ecosystem preservation and sustainability, they are a necessary part of the biosphere. They are estimated to make up nearly half of all living organisms. As a means of coping with the different environmental and competitive pressures they face, they've developed systems that allow them to adapt. It is man's greed for survival that has made disease-causing microbes particularly sensitive to antimicrobial agents. In response, these microbes have evolved resistance mechanisms to fend off the attack.

At the present time, the spread of antimicrobial resistance is a major concern to the global management of infectious diseases worldwide. When studying the mechanisms of resistance, it is crucial to understand how antimicrobial drugs work. With low or no influence on the host, antimicrobial medicines may target certain bacteria processes while having minimal or no effect on the host. Antimicrobial drugs have distinct mechanisms of action. Resistance to antimicrobials can only be understood by comprehending the processes by which they work and the chemical makeup of those agents. It is possible to further classify antimicrobial drugs in terms of how they impact bacteria's structure and how they influence its functions.

The array of antimicrobial compounds that microorganisms are being pummelling with is making

Table 6 — Preliminary *in vitro* antibacterial screening activity of HL and complexes **1–5**

Compd	Inhibition Zone (mm)					
	Staphylococcus aureus		*Salmonella typhi*		*Escherichia coli*	
	100 µg	200 µg	100 µg	200 µg	100 µg	200 µg
HL	–	+	+	+	+	+
$Rh(L)_2$, **1**	–	+	+	+++	++	++
$Co(L)_2$, **2**	+++	++	++	+	++	++
$VO(L)_2$, **3**	+	++	+	++	+	++
$Au(L)_2$, **4**	++	++	+++	++	++	++
$Pd(L)_2$, **5**	+++	+	++	++	++	++

+ = 5–10 mm, ++ = 11–20 mm, +++ = larger than 20 mm, – = no inhibition.

them more and more resistant. They accomplished this in a variety of ways, but principally based on the chemical composition of the antimicrobial agent and the methods by which the agents fought off the bacteria. Consequently, the processes of drug-resistance are dependent on the medications' inhibition of certain pathways as well as the organisms' ability to adapt certain pathways to circumvent those inhibitions and so live. There are two ways to define resistance. For medications that must enter the microbial cell in order to exert their effects, bacteria may have limited permeability to these agents due to differences in the chemical makeup of the drug and the membrane structures found in microbes. This is known as intrinsic or natural permeability. Normally vulnerable microorganisms develop methods of avoiding the drug's effect *via* acquired resistance.

Antibacterial screening results for ligand, HL, and complexes **1–5** are summarised in Table 6. *Staphylococcus aureus*, *Salmonella typhi*, and *Escherichia coli* bacterium strains were inoculated with the produced complexes and the ligand, HL, to test their *in vitro* antibacterial activity[12]. One standard 6.35-mm sterilised filter paper disc was put on an agar plate seeded with the test bacterium, and it was saturated with the compound (at 200 or 100 lg/mL in DMSO) using this approach[13]. For 24 h, the plates were kept at 37°C (Ref. 14). The inhibitory zone diameter (in mm) was utilised to calculate the activity[15], with streptomycin serving as the standard control[16]. When compared to the ligand, HL, the preliminarily discovered complexes **1–5** are found to be much more active[17]. Despite using larger concentrations, the overall activity of all the complexes was determined to be moderate[18]. This may be owing to the molecule's bulkiness, which hinders its mobility to the target cell or active site, despite the fact that all the complexes were produced as monomeric and four-coordinated metal (II) and metal (III) moieties, respectively[19].

Conclusions

The 2N-salicylidene-5-(*p*-aminophenyl)-1,3,4-thiadiazole ligand was effectively synthesised. Oxygen and nitrogen atoms in the ligand HL were used to coordinate five distinct metal ions, resulting in the matching complexes. Each of the complexes except for complex **2** and complex **3** had a tetrahedral or square pyramidal structure, and were all four-coordinated. Compared to the ligand, HL, preliminary *in vitro* antibacterial studies revealed that all of the complexes produced had modest activity against the tested types of bacteria.

Acknowledgment

The authors thank the Director of the Indian Institute of Chemical Technology, Hyderabad, as well as Kakatiya University's Department of Chemistry, Director of Center for Cellular and Molecular Biology Hyderabad, and Vaagdevi Degree and PG College, Hanamkonda, for delivering spectral data and biological activity.

Conflict of Interests

The authors declare no conflicts of interest.

Supplementary Information

Supplementary information is available in the website http://nopr.niscpr.res.in/handle/123456789/58776.

References

1 Ahmad A, Rafatullah M, Sulaiman O, Ibrahim M H & Hashim R, *J Hazard Mat*, 170 (2009) 357.

2 Ajmal M, Khan A H, Ahmad S & Ahmad A, *Water Res*, 32 (1998) 3085.

3 Nakamoto K, *Infrared of Inorganic and Coordination Compounds*, 6th edn, (John-Wiley, New York) (1997).

4 Hossain S, Zakaria C M, Haque M M & Zahan M K E, *International Journal of Chemical Studie*s, 4 (2016) 1.
5 Emad Y, Ahmed M, Al-Sammarrae K, Nadia S, Salimon J & Abdullah B, *Arabian J Chem*, 10 (2017) S1639.
6 Ahmed M F A & Yunus V M, *Orient J Chem*, 30 (2014) 111.
7 Yousif E, Adil H & Farina Y, *J Appl Sci Res*, 6 (2010) 879.
8 Barakat M A, *Arabian J Chem*, 4 (2011) 361.
9 Annapoorani S & Krishnan C, *Int J Chem Tech Res*, 5 (2013) 180.
10 Kumari G, Kumar D, Singh C P, Kumar A & Rana V B, *J Serb Chem Soc*, 75 (2010) 629.
11 Shaker S A, *Hindawi J Chem*, 7 (2010).
12 Bhanuka S & Singh H L, *Rasayan J Chem*, 10 (2017) 673.
13 Neelofar N, Ali N, Ahmad S, El-Salam N M A, Ullah R, Nawaz R & Ahmad S, *Trop J Pharm Res*, 15 (2016) 2693.
14 Elzahany E, Hegab K, Khalil S, Youssef N, *Aust J Basic Appl Sci*, 2 (2008) 210.
15 Figgis B, *Ligand Field Theory and its Applications*, 1st edn, (John-Wiley, New York) (2000).
16 Kim Y R, Kim H J, Kim J S & Kim H, *Adv Mater*, 20 (2008) 4428.
17 Zhou Y, Wang S X, Zhang K, Jiang X Y, *Angew. Chem*, 120 (2008) 7564.
18 Gondia N K, Priya J & Sharma S K, *Res Chem Intermed*, 43 (2017) 1165.
19 Thaker B T & Barvalia R S, *Spectrochim Acta A*, 112 (2013) 101.